

The Influence of Electroless Silver Deposition on Electrochemical Properties of the Steel Cathode Current Collector of Alkaline Batteries

M. Ghaemi^{1,*}, F. Makhlooghi², H. Adelhani³, M. Aghazadeh², H. M. Shiri²

¹ Department of Chemistry, Science Faculty, Golestan University, P.O. Box 49138-15739, Gorgan, Iran

² Department of Chemistry, School of Sciences, Tarbiat Modares University, P.O. Box 14115-175, Tehran, Iran

³ Department of Metallurgy, Materials Research School, NSTRI, P.O.Box 14395-836, Tehran, Iran

*E-mail: ghaemi_m@gau.ac.ir

Received: 6 August 2009 / Accepted: 11 January 2010 / Published: 31 January 2010

The influence of electroless silver layer on the electrochemical behavior of steel cathode current collector was examined in rechargeable alkaline MnO₂-Zn batteries. For that purpose, batteries were dismantled after various stages of charge/discharge cycles, followed by polarization measurements and morphological analysis of their steel collectors. The current collectors of spent batteries were used for construction of a new series of batteries. Results indicate that the formation of passive surface film on the steel current collector impairs the charge/discharge cycle performance of batteries. To overcome the difficulties, electroless silver coating on steel collector was proposed. SEM analysis has shown that, the surface defects density and accumulation of corrosion products on steel collector is higher than that of Ag coated collector. Furthermore, the second cycle discharge capacity and the rate of capacity fading of batteries with silver coated collectors were lower in comparison with batteries based on steel collector. Results of electrochemical impedance spectroscopy (EIS) have confirmed that the polarization resistance of steel current collectors is higher than that of the corresponding silver coated collectors.

Keywords: current collector, rechargeable MnO₂-zinc batteries, electroless silver

1. INTRODUCTION

The cycle life of Rechargeable Alkaline MnO₂-Zinc batteries (RAM) is affected by the internal resistance due to passive film formation occurring at the current collector/active material interface [1, 2]. This phenomenon is attributed to hindrance of the ion flux from the metal substrate to the

electrolyte, retarding the rate of electrochemical reactions [3]. In this regard, it is necessary that the current collector does not participate chemically or electrochemically in the electrode reactions due to possible galvanic effects and/or increase of the contact resistance. Hence, the choice of an adequate current collector is important for a proper functioning of the active material [4, 5].

Result of our previous work has shown that lowering the internal resistance and maintenance of a good electrical contact between active material and the anode current collector plays an important role in batteries' cycle life [6]. At the present time, steel, which possesses an anticorrosion oxide layer [7], is the preferred material as the cathode current collector in alkaline batteries. However, little attention has been paid to the fact that the corrosion of steel in alkaline environment may cause continuous capacity loss during charge/discharge cycling. According to the Pourbaix diagram, iron, the main component of the steel collector, is passivated under alkaline conditions by the presence of an oxide/hydroxide film [8]. However, poorly conductive iron oxide films may form on the surface of current collector in the course of charge/discharge cycling or during prolonged storage.

The internal resistance of the battery generally consists of the polarization resistance at the anode and cathode, the resistance of the electrolyte and electrical contacts and also the resistance of passive film formed on the current collector [9]. The latter resistance maybe reduced due to application of silver, which may contribute to an increase of the cycle performance of batteries under the same conditions of charge/discharge cycling.

In order to minimize the ohmic losses at the interface between the cathode and its current collector, steel collector has been coated by a thin layer of electroless silver. According to our knowledge, little information is currently available about the application of silver as current collector for alkaline batteries in published literature.

The results of this preliminary study suggest that the negative effect of the surface film formation and degradation of steel collector cannot be neglected. It is demonstrated that both the charge/discharge capacities and the cycleability of batteries could be improved by means of conductive silver coated on steel.

2. EXPERIMENTAL PART

Steel and Ag plated steel were investigated as to their corrosion behavior and their quality as cathode current-collectors. The battery grade steel collector is extracted from rechargeable pure energy alkaline batteries (Canada). According to X-ray fluorescence analysis (XRF), among other trace elements (Mn, Cl, P, Si, Al), Ni and Fe content of this material was 31 and 68 wt. %, respectively. Steel surface were ground with a fine emery paper and degreased with acetone before the experiments. Thereafter, electroless silver plating was carried out on steel surface using conventional bath technique [10, 11]. The produced collector materials, cut in circular with a geometric area of 0.785 cm^2 , were used for electrochemical charge/discharge cycling. All specimens were prepared just before cycling tests in laboratory designed batteries.

Potentiodynamic measurements were carried out by means of a Potentiostat-Galvanostat EG&G PAR 273A using an Hg/HgO reference electrode and Pt auxiliary electrode with a scan rate of $0.5 \text{ mV}\cdot\text{s}^{-1}$ in 9 M KOH solution. Anodic polarization measurements were performed with a scan rate of $0.25 \text{ mV}\cdot\text{s}^{-1}$ in 9 M KOH solution. The growth and morphological features of the passive films were analyzed by means of scanning electron microscopy (SEM) Oxford model LE0440I.

The electrochemical impedance measurements were performed using an EG & G model 273 potentiostat/galvanostat. An Hg/HgO electrode and a platinum electrode in KOH (9M) were used as reference and auxiliary electrodes, respectively. The working electrode (WE), in the form of disc was cut from steel and Ag-coated steel. Spectra were obtained at open circuit potential with a perturbing signal of 10 mV at a scan rate of 0.5 mVs^{-1} . The frequency span generally ranged from 1 kHz to 1 mHz.

2.1. Construction and preparations of batteries

The laboratory designed batteries were made of an upper cap and a lower case with a removable cathode current collector fitted at the bottom of the cathodic cap. The cell design is described in details elsewhere [12]. The cathode mixture consisted of electrolytic manganese dioxide powder (90 wt. % TOSOH, Hellas, Greece), graphite (9.5 wt. %) and carbon black (2.5 wt. %). Around 280 mg of cathodic mixture is required to make each compact cathode disc. Approximately 25–30 ml of 9M KOH was required to supply the necessary moisture for the production of discs. The cathode mixture was pressed at 5 t cm^{-2} by means of a special steel die and press device for 1 min. Approximately 200 mg of anodic powder was used to prepare the anodic gel. All batteries have been charged by voltage limited taper current (VLTC) method to 1.7V and discharged galvanostatically at a current density of $30 \text{ mA}\cdot\text{g}^{-1} \text{ MnO}_2$ to a cut-off voltage (COV) of 0.9V.

Table 1. Label of batteries, steel and Ag coated steel current collectors with their corresponding corrosion data.

No. of charge/discharge cycles	Label of Ag coated steel c. collector	Label of batteries	Label of Steel c.collector	Label of batteries	E_{corr} (steel c.collector)	I_{corr} (steel c.collector)
0	Ag0	BAG0	St0	BSt0	-475	630
2	Ag2	BAG2	St2	BSt2	-455	251
5	Ag5	BAG5	St5	BSt5	-380	126
15	Ag15	BAG15	St15	BSt15	-355	39.8
25	Ag25	BAG25	St25	BSt25	-350	79
40	Ag40	BAG40	St40	BSt40	-325	5.1

Based on polished steel current collectors (labeled as St0, table 1), some similar batteries were constructed (BSt0-batteries). The charge/discharge cycling of these batteries were disrupted after the 2th, 5th, 15th, 25th and 40th. Thereafter, all batteries were dismantled in order to remove their used cathode current collectors. These were carefully washed several times with distilled water to wipe the cathode mix and dried for a short time in dessicator. According to the number of charge/discharge cycling, the steel collectors of these used batteries have been labeled as St2, St5, St15, St25 and St40 respectively.

In order to study the effect of the formed surface passive film on the capacity fading of batteries, St5, St15, St25 and St40 were employed as cathode current collectors for a new series of fresh batteries. According to the used collector, this series of batteries have been labeled as BSt5, BSt15, BSt25 and BSt40, respectively. In a similar way, based on silver coated steel collector (Ag0), some batteries were constructed (BAG0-batteries). Charge/discharge cycling of BAG0 batteries were disrupted after the 2th, 5th, 15th, 25th and 40th charge/discharge cycling and their corresponding spent collectors labeled as Ag2, Ag5, Ag15, Ag25 and Ag40. After dismantling of the battery at various stages of charge/discharge cycling, Ag coated collectors were also carefully removed, washed and dried in a dessicator. These collectors were used for construction of a new series of fresh batteries: BAg2, BAg5, BAg15, BAg25 and BAg40 respectively.

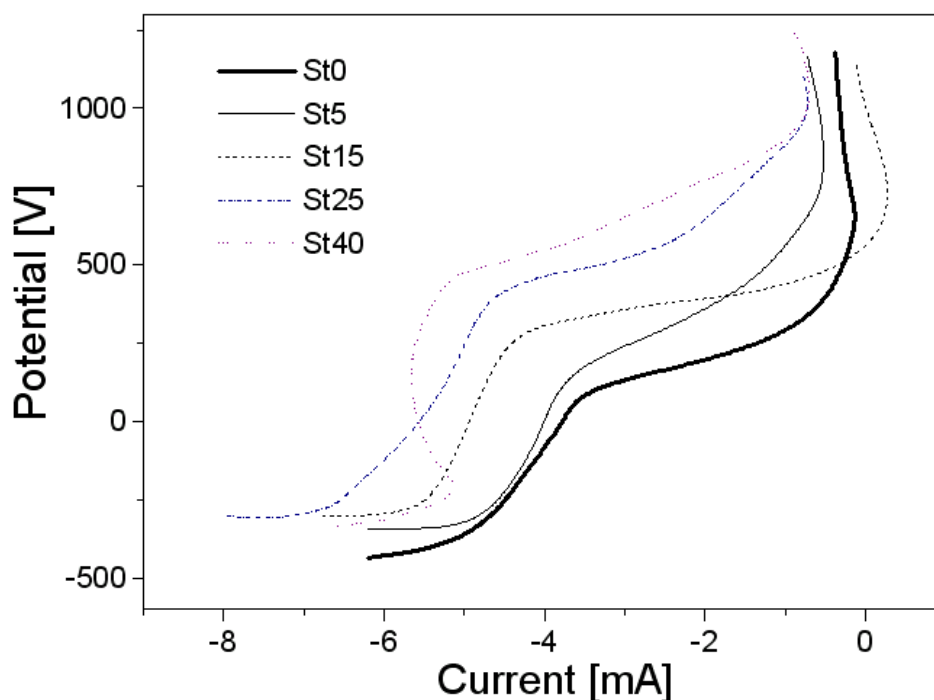


Figure 1. Anodic polarization curves of steel current collectors St0-St40 at a scan rate of $0.25 \text{ mV}\cdot\text{s}^{-1}$ in 9 M KOH.

3. POTENTIODYNAMIC AND CORROSION STUDY MEASUREMENTS

Anodic polarization curves were recorded to compare the behavior of steel collector at different stages of charge/discharge cycling. The potential has been scanned from open circuit potential (OCP) to 1250 mV with a scan rate of $0.25 \text{ mV}\cdot\text{s}^{-1}$ in 9 M KOH solution. The anodic peak is followed by a broad passive region extending up to 500 mV (Fig. 1). At these anodic potentials, active metal dissolution takes place and the anodic polarization curve exhibits a passivation plateau. As the electrode potential exceeds the breakdown potential, with a value of nearly +100 mV for St0, a steep increase in the current is observed. A second region of passivation is observed for St0 at potentials higher than 300 mV due to formation and development of surface coverage by passive films. The start potential of the second passivation is also increased for all St-samples with increasing number of cycling. As could be seen in the graph, the breakdown potential shifts towards more positive values and the passive potential range is increased with increasing number of cycling. Simultaneously, the anodic potential shifts to more positive values accompanied with a reduction in anodic current. These results are in good agreement and support the assumption that the extent of passivity is increased with increasing number of charge/discharge cycling. This may be attributed to higher concentration of oxygen containing species in the passive film.

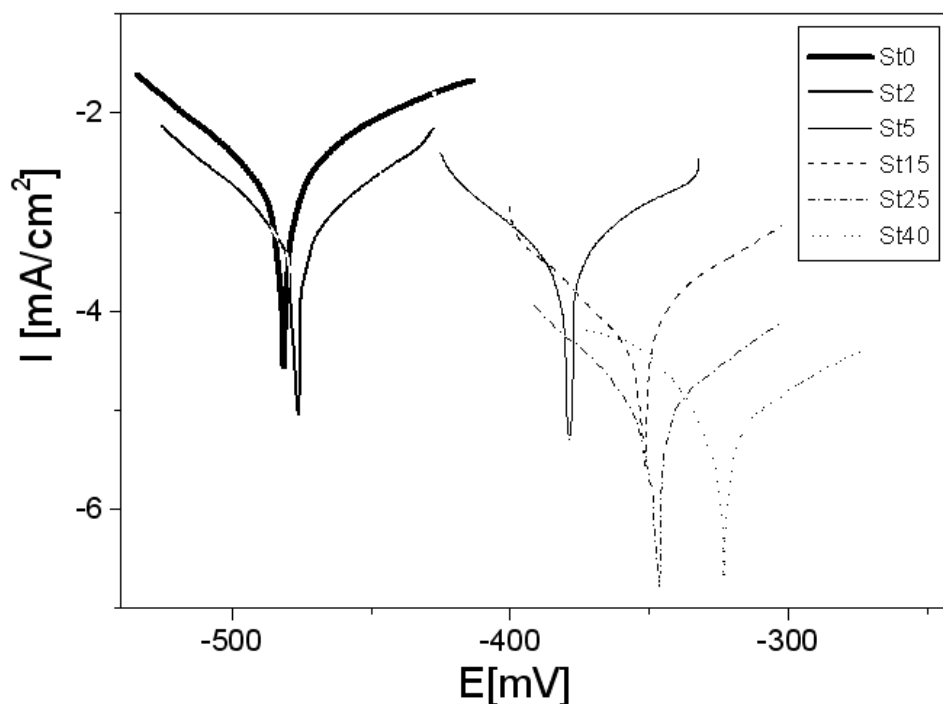
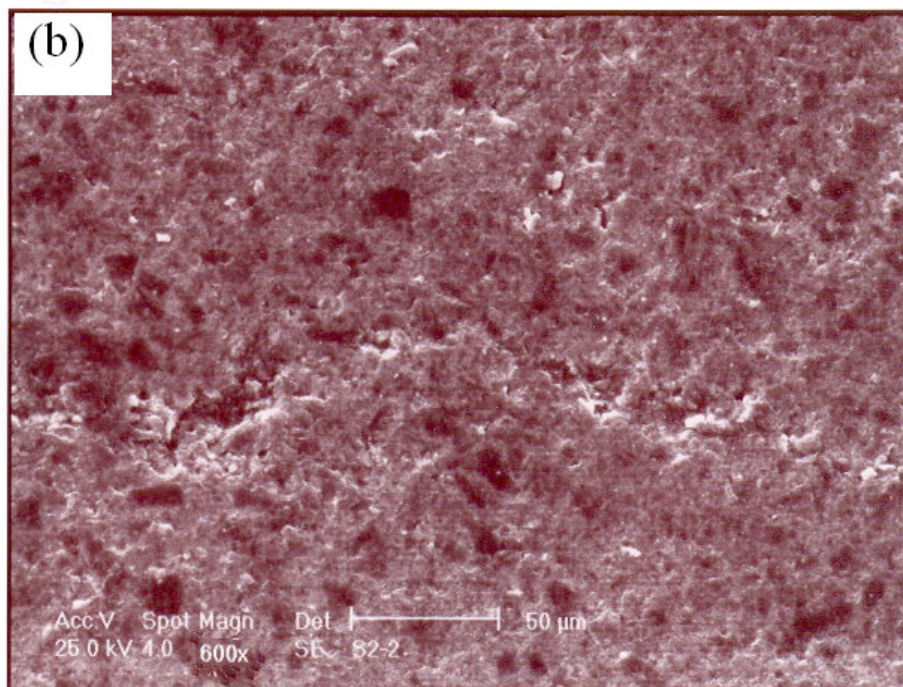
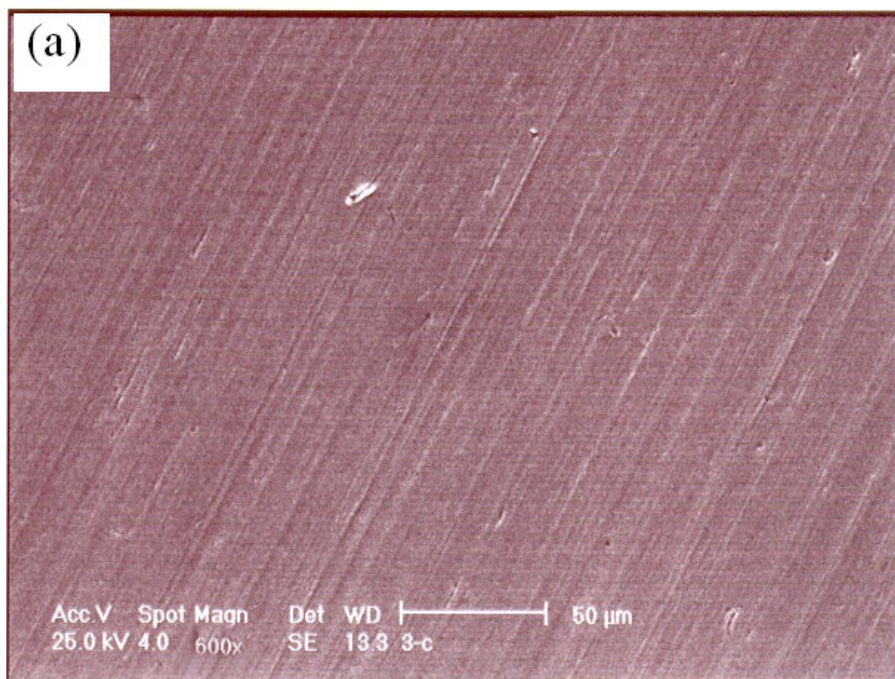


Figure 2. Potentiodynamic polarization curves recorded for steel current collectors St₀-St₄₀ at a scan rate of $0.5 \text{ mV}\cdot\text{s}^{-1}$ in alkaline in 9M KOH.

The electrochemical activity and the tendency of steel cathode current collector to passivity were studied after going through the various steps in the charge/discharge cycling. For this reason, potentiodynamic polarization technique was also used to study the tolerability of this material as current collector (Fig. 2). The point of intersection of the tangent lines to the cathodic and anodic branches at the corrosion potential yields i_{corr} . Resulting electrochemical parameters are tabulated in table 1. As compared to the steel collector of spent batteries, St0 represents a much more reactive state in this environment as it exhibits a significantly more negative corrosion potential and higher magnitude of current density. With increasing number of charge/discharge cycling, the corrosion potentials are shifted towards more positive values, where an apparent decrease in corrosion current densities can also be detected. These implications give a strong indication that the corrosion process, performed even during the initial stages of cycling, causes the passivity of collector *via* formation of a surface oxide layer. Polarization resistance can be associated with corrosion processes (anodic oxidation of steel with oxygen reduction) as well as with other accompanied processes, e.g. accumulation of corrosion products. As we will see in section 5, this results in significant increase of voltage delay and loss of battery capacities.

4. SURFACE CHARACTERIZATION OF CORROSION FILMS GROWN ON THE CURRENT COLLECTOR

SEM was used to gain a deeper insight into the morphology of steel surfaces formed at various steps of the cycling procedure. Figs. 3a -3d show surface micrographs of freshly polished steel current collector and its surface after 2th, 25th and 40th charge/ discharge cycle. As could be seen in the graph, due to accumulation of corrosion products, surface roughness and surface defects increased rapidly with proceeding cycling. These unavoidable defects destroy the whole surface and thus initiate the corrosion. In such a surface with complicated composition and structures, all the electrochemical interfaces do not contribute equally to the charge transfer. In fact, these phenomena reduce the current distribution, causing progressive lowering of capacities. Fig. 4a shows surface micrographs of freshly deposited Ag on the steel current collector surface (Ag0) and its surface after various stages of cycling procedure (Fig 4b-4d). These micrographs confirm that cycling of the batteries leads to the formation surface films on the Ag current collector as well. The formed passive films on both types of collectors show the characteristics of an amorphous film; however, Ag surface appears more homogeneous with a lower amount of accumulated corrosion products and reduced number/size of surface defects/cracks. As could be seen in Fig. 4b, this film presents scratches, but these are visible after the second cycle. This is indicative of the small thickness of the formed passive film after the second cycle. As could be seen in the graph, the film becomes irregular and uneven at later 25th and 40th cycle; indicating the surface morphology changes with a visible increase of roughness and thickness of formed passive oxide-layer.



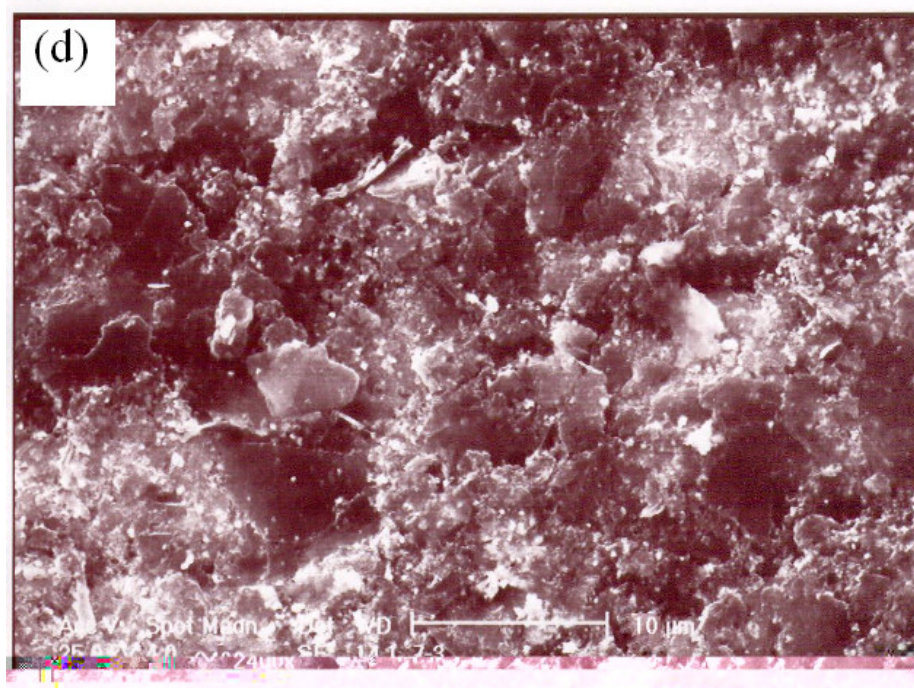
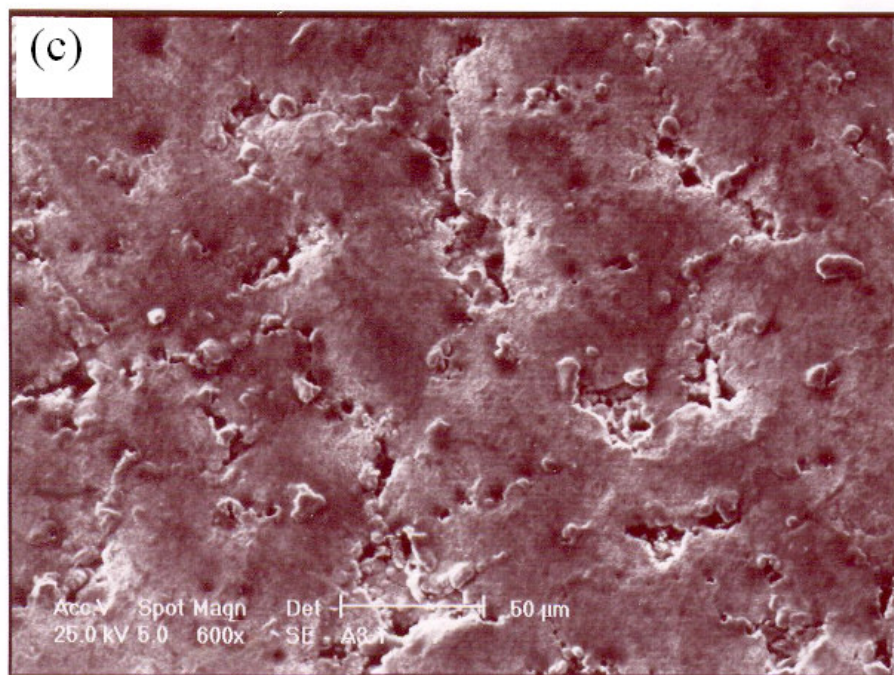
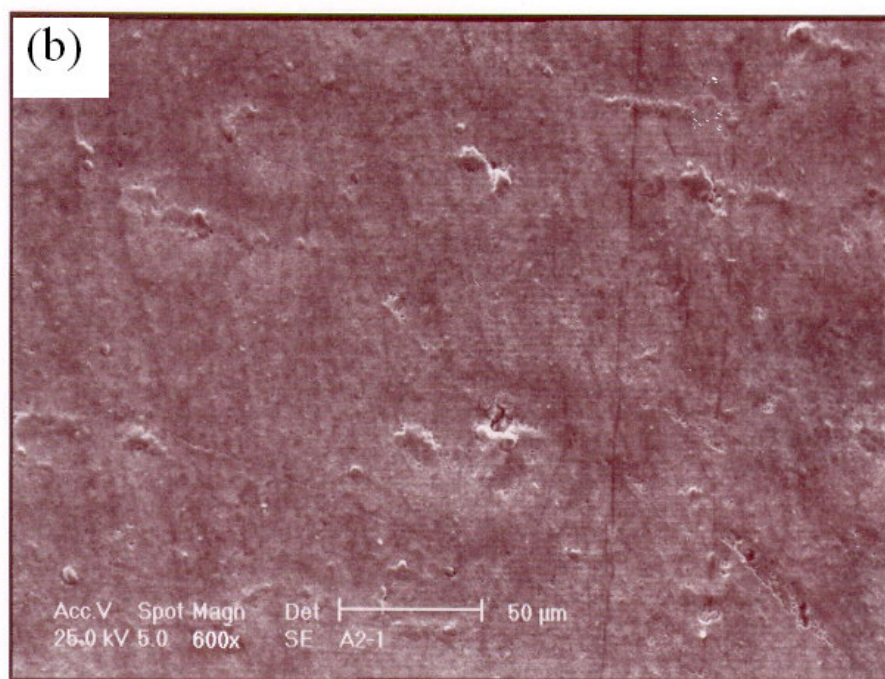
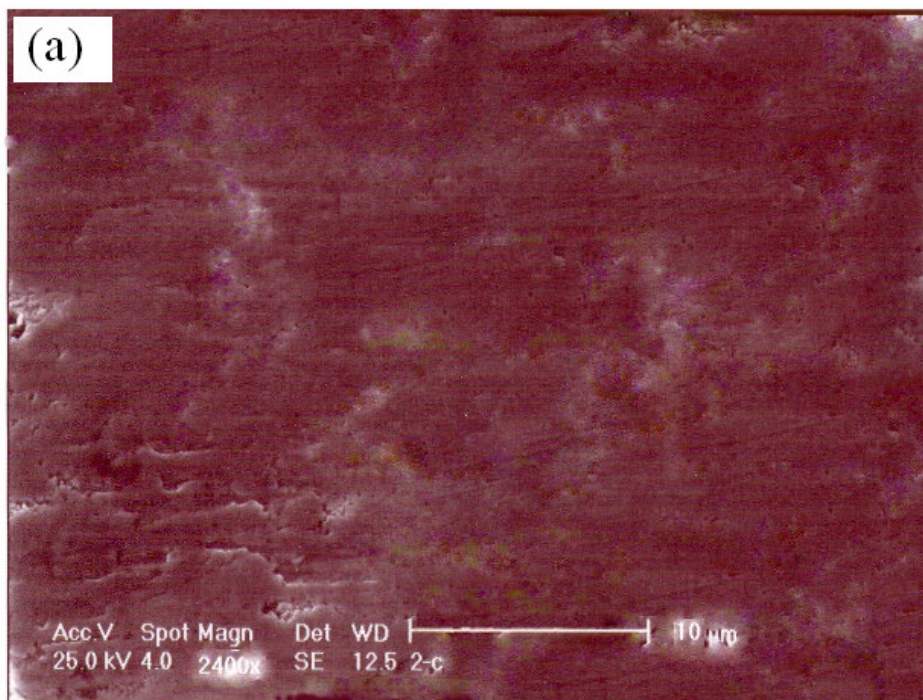


Figure 3. SEM micrographs of steel current collectors: St0 (a), St2 (b), St15 (c) and St40 (d).



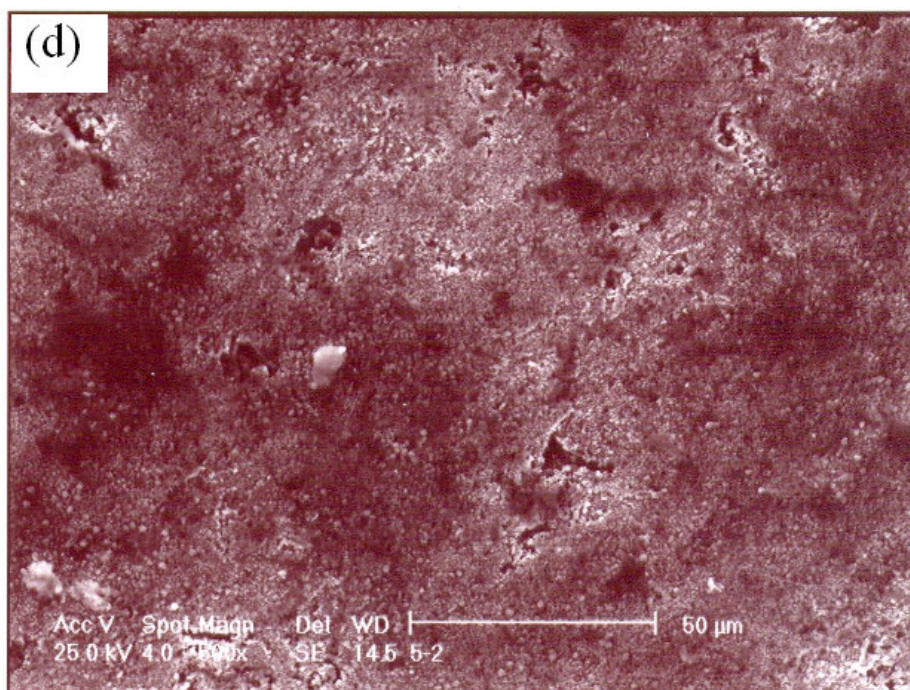
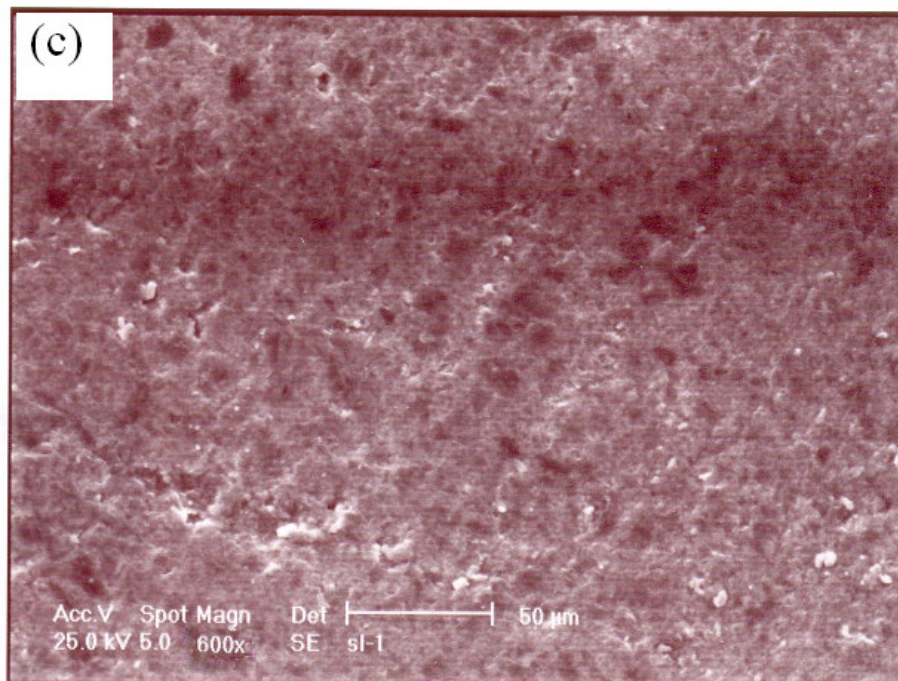


Figure 4. SEM micrographs of Ag coated steel current collectors: Ag0 (a), Ag2 (b), Ag15 (c), and Ag40 (d).

5. CHARGE/DISCHARGE CYCLING OF BATTERIES

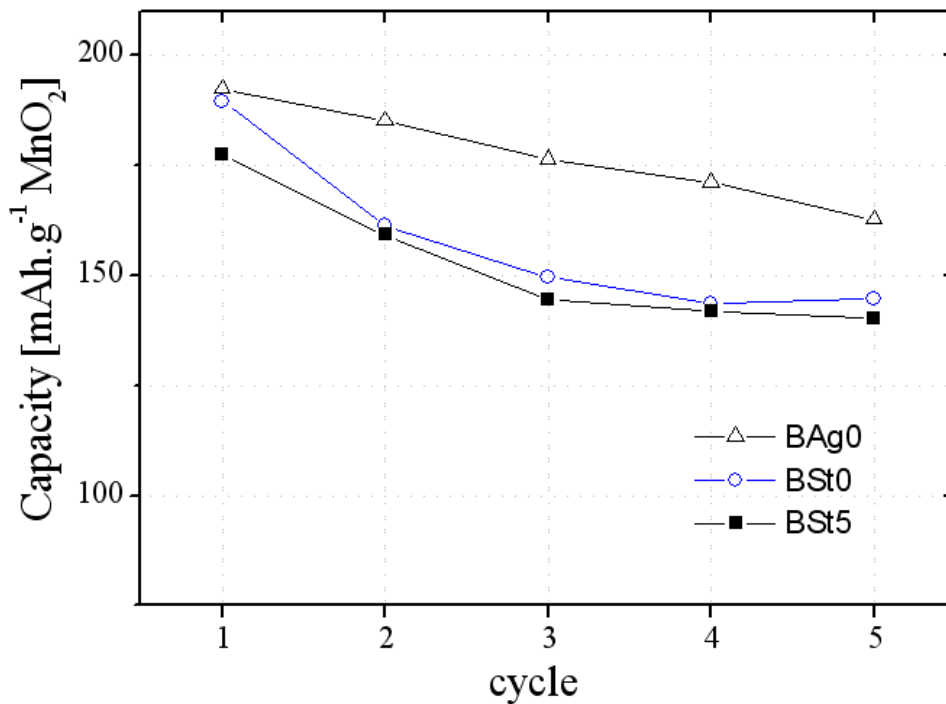
The cycle performance of BSt0 batteries are evaluated by continuous charge/discharge cycling up to 40 cycles. The results are illustrated in Figs. 5a-5d, where the charge and discharge capacities are reported upon repetitive cycles. For the sake of clarity, the average result is shown for only one BSt0 battery, but they were reproduced for several batteries. As could be seen in the figure, BSt0 was able to deliver a first cycle capacity of about $190 \text{ mAh.g}^{-1} \text{ MnO}_2$ and after 40 cycles the delivered capacity was still above 40 mAh.g^{-1} . In comparison, BSt40 deliver a first cycle capacity of just 158 mAh.g^{-1} , which was decreased to nearly 30 mAh.g^{-1} after 40 cycles. As could be seen Fig. 5, the corresponding first cycle capacities decreases in the order: BSt0 > BSt5 > BSt15 > BSt25 > BSt40. Fig. 6 shows that, the cumulative capacity of BSt0 decreases to more than 10% of its original value when using BSt15, BSt25 and BSt40. The obtained data confirmed the results of SEM micrographs that cycling leads to some deterioration in the current collector. With this approach, we ensure, detrimental phenomena that impair the batteries performance are easy to detect and study.

As could be seen in Fig. 5, BAg0 shows higher capacities after the first cycle and the Open Circuit Voltages (OCV) of these batteries were in average 100 mV higher than the corresponding BSt0 and other steel based batteries. In the second cycle, the capacity of BSt0 is reduced to more than 13% of that of BAg0. After 40th cycle, the discharge capacities of both batteries approach to a value of 45 mAh.g^{-1} (Fig. 5d). Fig. 6 shows clearly, that the cumulative capacity of BSt0 is significantly lower than that of BAg0. The difference in the cycle performance measured for both BSt0 and BAg0 batteries correlates well with the SEM morphological observations. The physico/chemical properties of this impure material depend on the current density and the time allowed for charging.

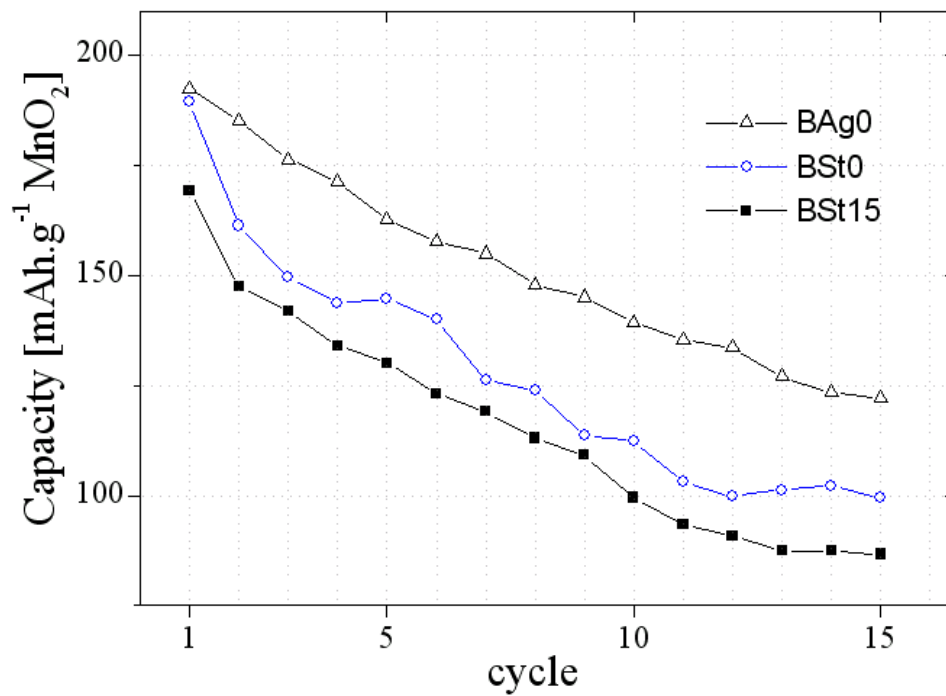
The higher cycle performance of batteries with silver coated collectors suggests that microscopic distribution of the conductive silver contributes to a more homogeneous current distribution due to higher conductivity, which can transmit electrons smoothly from the MnO_2 surface to the collector. Fig. 6 shows that differences in the cycle performance between BAg40 and BAg0 was lower compared to that between BSt40 and BSt0, indicating the beneficial effect of the used silver coated steel current collectors.

It is reasonable that other factors may also contribute to the capacity loss of Ag-based batteries at higher cycles. In view of the fact that Ag_2O and AgO are the predominant oxides of Ag in high-pH solutions, it is reported that even when the product is AgO , there are indications that electrolytically prepared AgO has some amounts of metallic silver mixed with it [13]. In an alkaline solution, a dissolution of Ag in the form of $[\text{Ag}(\text{OH})_2]$ has also been reported [14, 15]. Metallic silver seems to be able to make the electrode sufficiently conductive to show optimal behavior in discharge process. In this relation, it is reported that the presence of dispersed silver particles on the surface of the manganese dioxide can reduce the concentration of free hydroxyl groups or the formation of oxyhydroxyl passive intermediates [16]. This may affect the activity of the cathode material *via* its phase transformation and/or structural degradation [17, 18]. For this reason, the influence of the passive film on the electroactive material must be further studied in details.

(a)



(b)



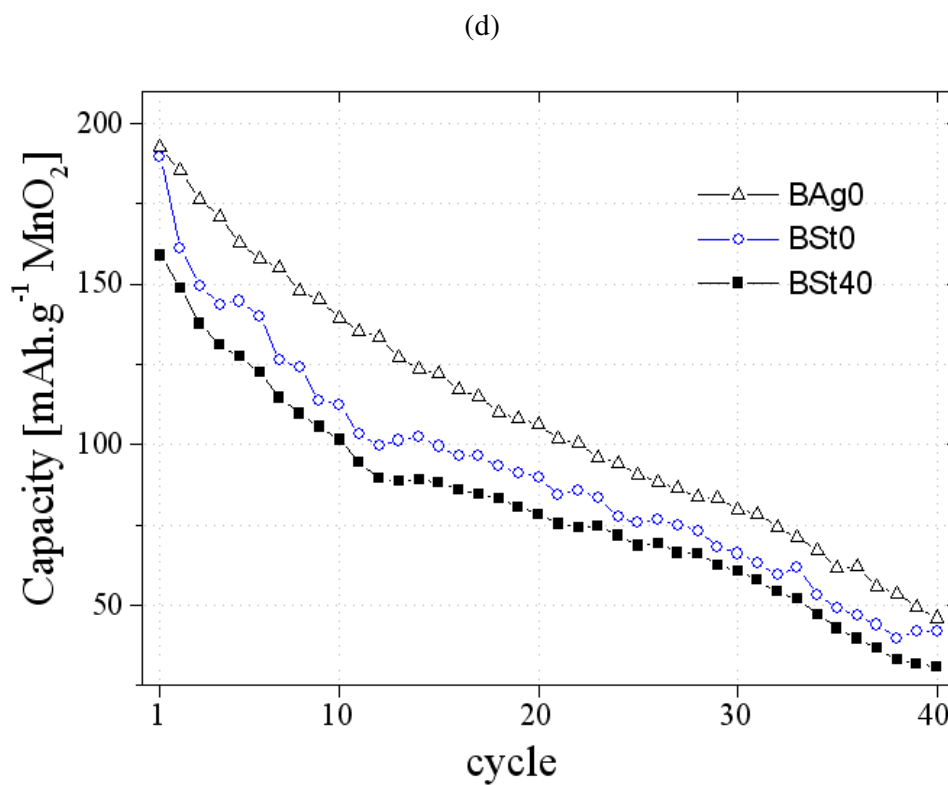
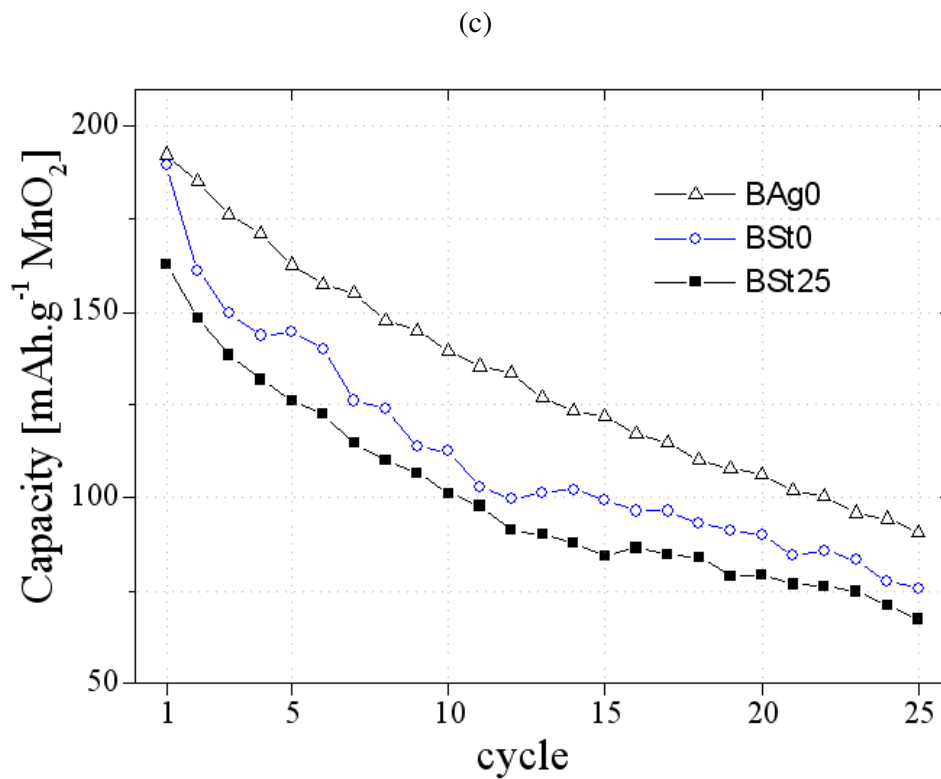


Figure 5. Cycle efficiency of batteries based on unused current collectors: (polished) steel collector (BSt0), as-deposited silver-coated steel (BAg0) and other batteries: BSt5, BSt15, BSt25 and BSt40 based on used current collectors.

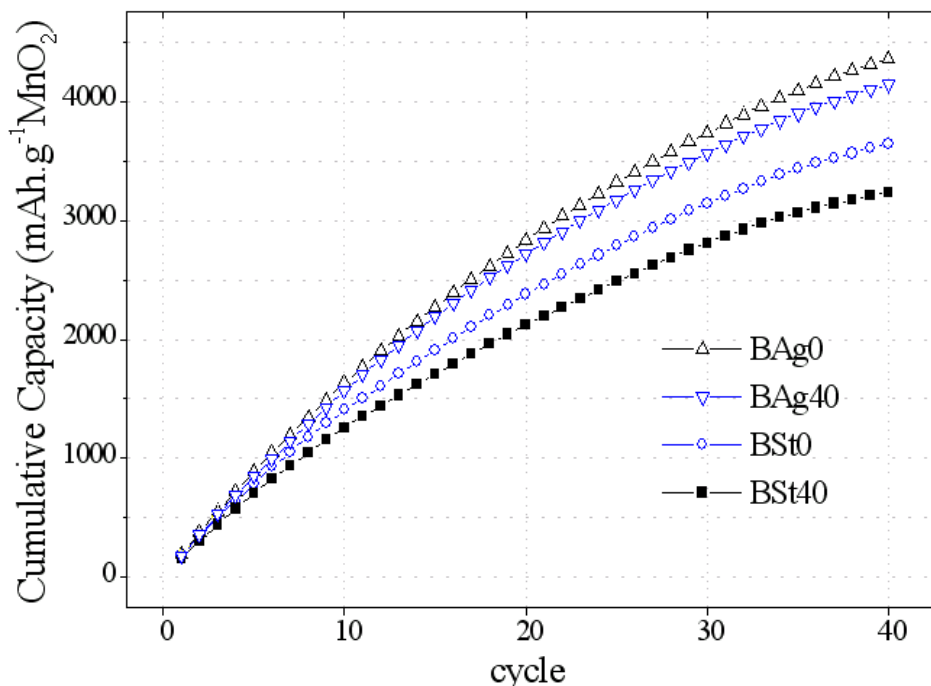


Figure 6. Cumulative capacities of batteries BAg0, BSt0 in comparison with other steel based batteries BSt5, BSt15, BSt25 and BSt40, cathode current collectors.

6. ELECTROCHEMICAL IMPEDANCE MEASUREMENTS

Impedance measurements were done for steel and Ag-coated steel collectors taken from the cells after various charge/discharge cycles. There are two depressed semicircles at high and mid frequencies, corresponding to the responses of two different processes. The first semicircle at high frequency was magnified and given in small window within the Nyquist plot (Fig. 7). This is representing the charge transfer process at collector/solution interface which could be calculated by extrapolation of the semicircle on the real impedance axis. The calculated charge transfer resistance ranging from 60 Ω for St0 to 420 Ω for St40. The second larger semicircle at lower frequency may be attributed to a much higher resistance of the passive oxide layer formed on St0, St5, St15 and St40 in the order of 1950, 22400, 29450 and 41560 Ω respectively. This suggests that the total interfacial resistance and/or the thickness of the passive film increased as cycling continued. The curves in Fig.8 show that the magnitudes of impedance for Ag-collector series are much lower than that of the untreated steel collector. The charge transfer resistance (R_{ct}), increased from 4859 Ω for Ag0 to 5980 Ω after 40th cycle (Ag40). This implies that electroless silver lead to a faster charge transfer in the electrode/solution interface in comparison with the corresponding R_{ct} values of St series.

It is proper to mention, that impedance studies of this part of a half cell gives only a partial cell resistance and could not be contributed to the whole positive electrode resistance. The overall cathode impedance cannot be found out unless the active material (MnO_2)/collector interface studies were made.

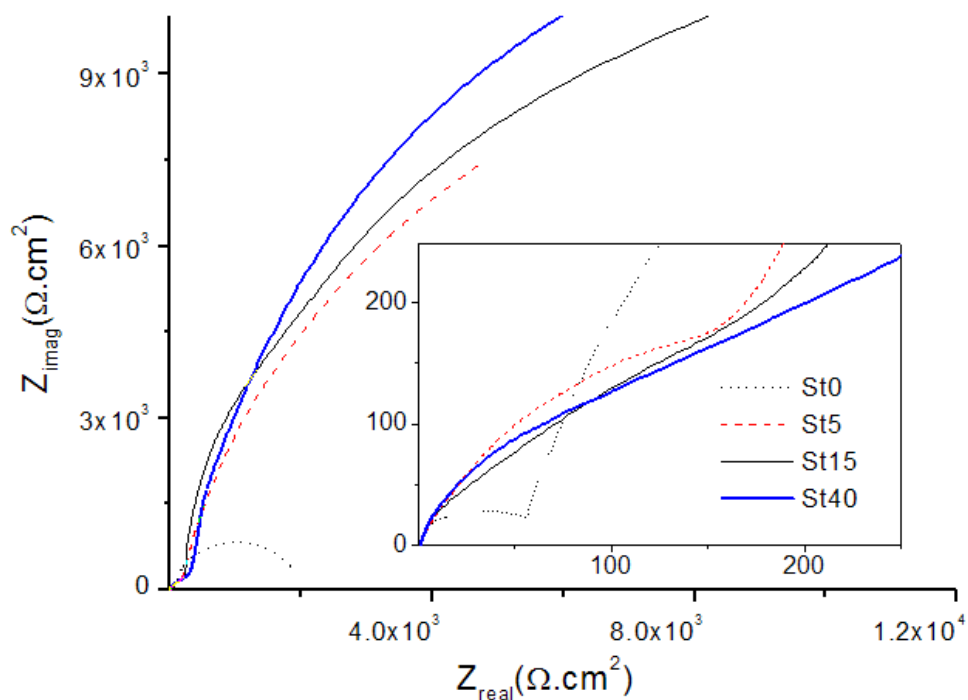


Figure 7. Nyquist plots for a polished steel current collector (St0), after cycle 5 (St5), after cycle 15 (St15) and after cycle 40 (St40)

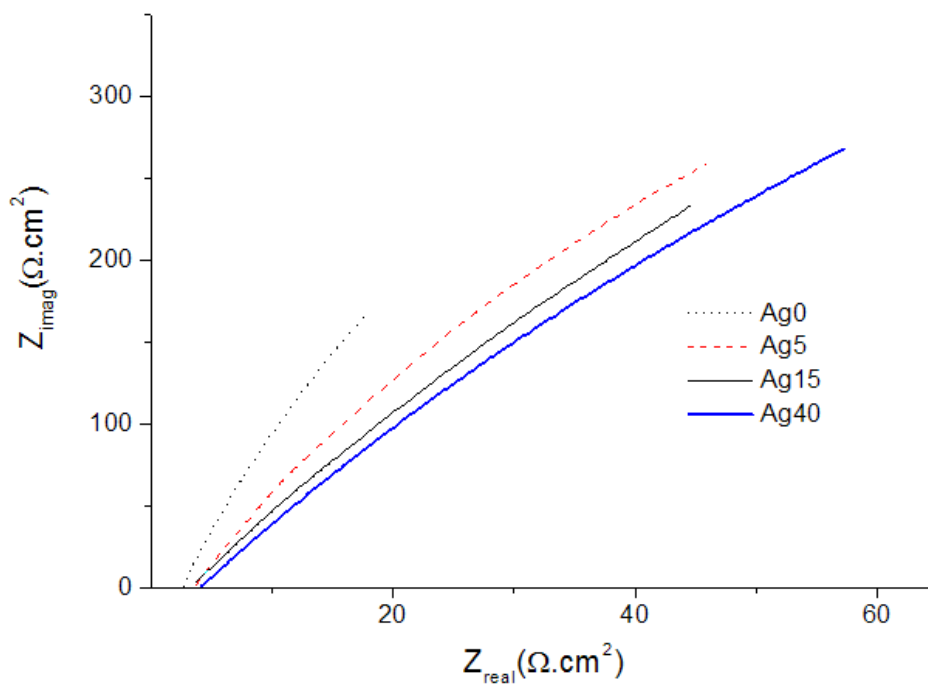


Figure 8. Nyquist plots for the as-deposited Ag coated steel current collector (Ag0), after cycle 5 (Ag5), after cycle 15 (Ag15) and after cycle 40 (Ag40)

7. CONCLUSIONS

The contact of the manganese dioxide cathode to the inside surface of the steel container of alkaline MnO_2/Zn batteries causes passivation of the steel current collector. Potentiodynamic measurements for steel cathode current collectors showed a shift in corrosion potential (E_{corr}) to less negative values with proceeding cycling. The experimental results from laboratory designed batteries have revealed that the considerable fast kinetics of corrosion and degradation of steel could be considered as a limiting factor for increasing voltage delay and decrease in electrochemical capacities. Our results have shown that the cycle performance of batteries becomes better with silver coated steel collectors. It is possible that silver oxide particles, which are formed during charging of the battery, became more conductive on discharge. Furthermore, the improve in charge/discharge cycling could be attributed to the reduced formation of surface defects, lower accumulation of corrosion products and reduced polarization of Ag coated steel current collector.

References

1. F. Beck, P. Rüetschi, *Electrochim. Acta* 45 (2000) 2467
2. I. Serebrennikova, *J. Electrochem. Society*, 154 (2007) 487
3. S. Virtanen, P. Schmuki, H.S. Isaacs, *Electrochim. Acta* 47 (2002) 3117
4. M. Guillodo, P. Vernoux, J. Fouletier, *Solid State Ionics* 127 (2000) 99
5. S. R. Narayanan, *J. Power Sources*, 34 (1991) 13
6. M. Ghaemi, R. Amrollahi, F. Ataherian, M. Z. Kassae, *J. Power Sources*, 17(2003) 233
7. Jun-Nan Nian, Hsisheng Teng, *J. Phys. Chem. B* 109 (2005) 10279
8. M. Pourbaix, *Atlas of Electrochemical Equilibrium in Aqueous Solutions*, Pergamon Press, Oxford, 1966, p. 307
9. Shalini Rodrigues, N. Munichandraiah, A.K. Shukla, *J Solid State Electrochem* 3(1999) 397
10. H. Chang, C. H. Pitt, G. B. Alexander, *J. Mater. Sci.*, 28 (1993) 5207
11. E. Norkus, *Surf. Coat. Technol.*, 82 (1996)165.
12. M. Ghaemi, Z. Biglari, L. Binder, *J. Power Sources*, 102 (2001) 29
13. T. P. Dirkse, *Electrochim. Acta* 35 (1990) 1445
14. S. B. Emery, J. L. Hubble, M. A. Darling, D. Roy, *Materials Chemistry and Physics* 89 (2005) 345
15. J.E. Garland, C.M. Pettit, D. Roy, *Electrochim. Acta* 49 (2004) 2623
16. W. Gac, G. Giecko, S. Pasieczna-Patkowska, T. Borowiecki, L. Kepiński, *Catal. Today*, 137(2008) 397
17. X. Tang, J. Chen, Yongg. Li, Yong Li, Y. Xu, W. Shen, *Chem. Eng. J*, 118 (2006)
18. Wojciech Gac, *App. Catal. B: Environmental* 75 (2007) 107